Rangin, C., Silver, E., von Breymann, M. T., et al., 1990
Proceedings of the Ocean Drilling Program, Initial Reports, Vol. 124

14. SITE 771[1]

Shipboard Scientific Party[2]

HOLE 771A

Date occupied: 31 December 1988

Date departed: 2 January 1989

Time on hole: 1 day, 15 hr, 30 min

Position: 08°40.69'N, 120°40.78'E

Bottom felt (rig floor; m, drill pipe measurement): 2870.0

Distance between rig floor and sea level (m): 11.30

Water depth (drill pipe measurement from sea level, m): 2858.7

Total depth (rig floor; m): 3174.1

Penetration (m): 304.1

Number of cores (including cores with no recovery): 18

Total length of cored section (m): 169.0

Total core recovered (m): 90.0

Core recovery (%): 53.2

Oldest sediment cored:
Depth (mbsf): 233.9
Nature: nannofossil clay and marl
Latest age: middle Miocene
Measured velocity (km/s): 1.62

Hard rock:
Depth (mbsf): 303.0
Nature: basaltic lava flows
Earliest age: late early Miocene
Measured velocity (km/s): 3.55

Principal results: Two lithologic units were distinguished at Site 771: a nannofossil marl and clay, overlying massive lapillistone, tuff, and basalt flows.

Unit I (100–233.9 mbsf) is middle Miocene to late Pliocene in age, and consists of nannofossil clay and marl with rare, thin carbonate turbidites. The material also contains minor silt-size volcanic detritus. Dispersed volcanic ash is found in the lower 30 m of Unit I, and its concentration increases in the lower 2 m.

Unit II (233.9–303.0 mbsf) is late early to early middle Miocene in age. It consists of volcaniclastic strata underlain and capped by basaltic lava flows. Thin-bedded coarse to fine tuffs occur below the upper basalt, but the dominant volcaniclastic rock is massive and structureless lapillistone.

The intercalation of flows and pyroclastic deposits implies proximity to a volcanic vent or set of vents. The hemipelagic marlstone just above the upper basalt is evidence for submarine eruption of the lavas. The boundary between Units I and II represents a rapid transition from volcaniclastic to hemipelagic sedimentation in early middle Miocene time. The major increase in carbonate content of the cores in Sites 768, 769, and 771 near the end of the Pliocene indicates a rapid drop in the CCD.

Table 1. Coring summary, Site 771.

Core no.	Date (Jan. 1989)	Time (UTC)	Depth (mbsf)	Cored (m)	Recovered (m)	Recovery (%)
124-771A-						
1R	1	0030	100.0–109.6	9.6	3.17	33.0
2R	1	0245	144.7–154.6	9.9	2.55	25.7
3R	1	0330	154.6–164.2	9.6	3.80	39.6
4R	1	0415	164.2–173.9	9.7	1.50	15.4
5R	1	0445	173.9–183.6	9.7	0.30	3.1
6R	1	0530	183.6–193.2	9.6	9.85	102.0
7R	1	0620	193.2–202.9	9.7	2.74	28.2
8R	1	0710	202.9–212.6	9.7	5.15	53.1
9R	1	0745	212.6–222.3	9.7	7.06	72.8
10R	1	0825	222.3–232.0	9.7	9.09	93.7
11R	1	0930	232.0–241.7	9.7	2.64	27.2
12R	1	1050	241.7–251.3	9.6	2.90	30.2
13R	1	1145	251.3–261.0	9.7	2.90	29.9
14R	1	1300	261.0–265.5	4.5	3.15	70.0
15R	1	1520	265.5–275.1	9.6	6.51	67.8
16R	1	1700	275.1–284.8	9.7	9.36	96.5
17R	1	1840	284.8–294.4	9.6	8.65	90.1
18R	1	2210	294.4–304.1	9.7	8.65	89.2
Coring totals				169.0	89.97	53.2

Note: Depths are drill-pipe measurements corrected to sea level.

BACKGROUND AND OBJECTIVES

Site 771, on the Cagayan Ridge (Fig. 1), was designed to complement Site 769. The major objectives of this site were (1) to date precisely the cessation of volcanism along the Cagayan Ridge and (2) to investigate the nature of the acoustic basement.

The age of the cessation of volcanism has been considered to be related either to the collision of this ridge with the rifted continental margin of China (North Palawan–Reed Bank block), or to the isolation of the Cagayan Ridge as a remnant volcanic arc during the opening of the Sulu Basin. Drilling at Site 769 has revealed bioturbated massive clay overlying massive unstratified coarse tuff and lapillistone. Because of the lack of age controls for these volcaniclastic rocks, the time period between the cessation of volcanic activity and the deposition of the massive clay is not precisely known. Drilling the clay/volcaniclastic interface at another site sufficiently spaced from the first could test the synchroneity of volcanic cessation along the Cagayan Ridge.

The petrological signature of the volcanic debris present in the mass flows drilled at Sites 768 and 769 are different. At Site 768 it is dominantly rhyolitic to dacitic in composition whereas at Site 769 these volcanic rocks are andesitic to basaltic. These contrasts have raised concerns of whether the Miocene volcanic sources for these deposits were the same. Drilling immediately northwestward of Site 768 was planned to test more accurately the parentage of the volcaniclastic rocks of the Cagayan Ridge relative to those of the Sulu Basin.

Site Selection

The proposed site is located on the eastern flank of the Cagayan Ridge, 50 nmi northwest of Site 768, on a large plateau

[1] Rangin, C., Silver, E., von Breymann, M. T., et al., 1990. *Proc. ODP, Init. Repts.*, 124: College Station, TX (Ocean Drilling Program).
[2] Shipboard Scientific Party is as given in the list of participants preceding the contents.

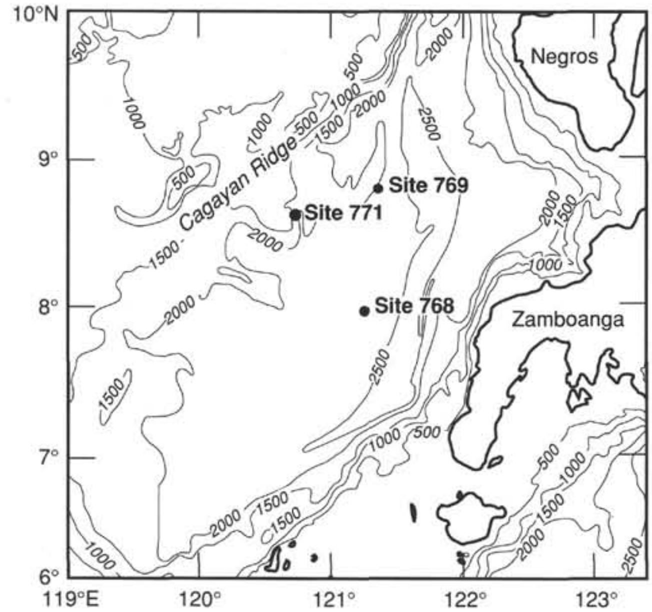

Figure 1. Location of Site 771 on the Cagayan Ridge.

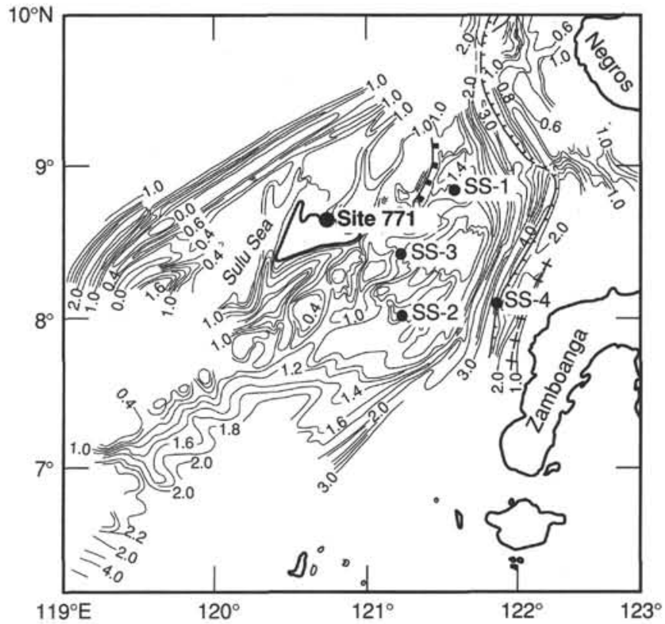

Figure 2. Reflection time map of the seafloor-basement interval (Hinz et al., BGR unpubl. rept. 103.463, 1988) showing the flat acoustic basement drilled at Site 771. Contour interval in seconds of two-way traveltime.

blanketed by a 0.3–0.5-s thickness of a fairly transparent layer (Fig. 2). This flat acoustic basement has been identified over a large area. Consequently, the results obtained by drilling at Site 771 are considered to be regionally representative.

The time for drilling was limited to 1.5 days; therefore, rotary core barrel (RCB) coring after washing the uppermost part of the section was planned for this site.

OPERATIONS

The new site lay about 38 nmi west-southwest of Site 769. The transit, by way of Basilan Strait, and the survey were completed in 25.5 hr, and the beacon was launched at 1330 hr (UTC), 31 December 1988.

Hole 771A

No "mud-line" core was requested, and seafloor sediments were extremely soft. The water depth determination of 2859 m below sea level (mbsl) was a compromise made on the basis of the corrected precision depth recorder (PDR) reading of 2867 and a somewhat deeper, but very subtle, weight indicator value. Spud time was 2200 hr (UTC), 31 December 1988.

The hole was drilled to 100 mbsf before the first spot core was taken. Continuous RCB coring began after further drilling to 145 mbsf. The sediments were marls and clays similar to those at Site 769 and were quite soft to 240 mbsf, where the much harder volcanic sequence was encountered. It was cored continuously to 304.1 mbsf, when coring was ended. We had reached our scientific goals, and operating time for the leg had expired.

The ship was underway for the final transit to Manila at 0500 hr (UTC), 2 January 1989.

LITHOSTRATIGRAPHY

Sedimentary Units

The hole drilled at Site 771 penetrated 303.05 m of sedimentary and volcanic rock. The hole was washed down to 100 mbsf, and one spot core was taken between 100 and 109.6 mbsf. After washing down to 144.7 mbsf, the hole was continuously cored to total depth (TD).

Two lithologic units were distinguished on the basis of visual description and smear slide analyses of the recovered cores (Fig. 3 and Table 2). Unit I is made up of nannofossil clay and nannofossil marl from 100 to 233.91 mbsf, and Unit II consists of massive lapillistone, tuff, and basalt flows between 233.91 and 303.05 mbsf.

Unit I

Depth: 100–233.91 mbsf
Interval: Core 124-771A-1R to Section 124-771A-11R-2 at 41 cm
Thickness: 133.91 m
Age: middle Miocene to late Pliocene

Unit I consists of clay with nannofossils, nannofossil clay, and nannofossil marl, which are interpreted as mixtures of hemipelagic clay and pelagic biogenic carbonate.

The upper part of Unit I is only represented in Core 124-771A-1R (upper Pliocene), which contains nannofossil clay with rare thin carbonate turbidites. The nannofossil clay is greenish gray with mottling caused by bioturbation. It is composed of clay, nannofossils, and minor silt-size volcanic detritus (plagioclase, glass, and lithic fragments). Interbedded with the nannofossil clay are rare thin to medium beds of nannofossil marl with foraminifers. These light greenish gray beds have sharp bases and gradational tops and are composed of clay, nannofossils, foraminifers, and small amounts of volcanic silt. They are interpreted as beds of pelagic/hemipelagic sediment redeposited by turbidity currents.

From Core 124-771A-2R to the base of the unit (lower Pliocene to middle Miocene), there is an irregular downward increase in the proportion of pelagic carbonate accompanied by an increase in induration. The sequence varies from clay with nannofossils in the upper part to nannofossil marlstone near the base. These lithotypes are primarily light to dark greenish gray and are massive, with few distinct bedding surfaces. Color mottling is present throughout the sequence, indicating a slight to moderate degree of bioturbation, though few distinct burrow traces are evident.

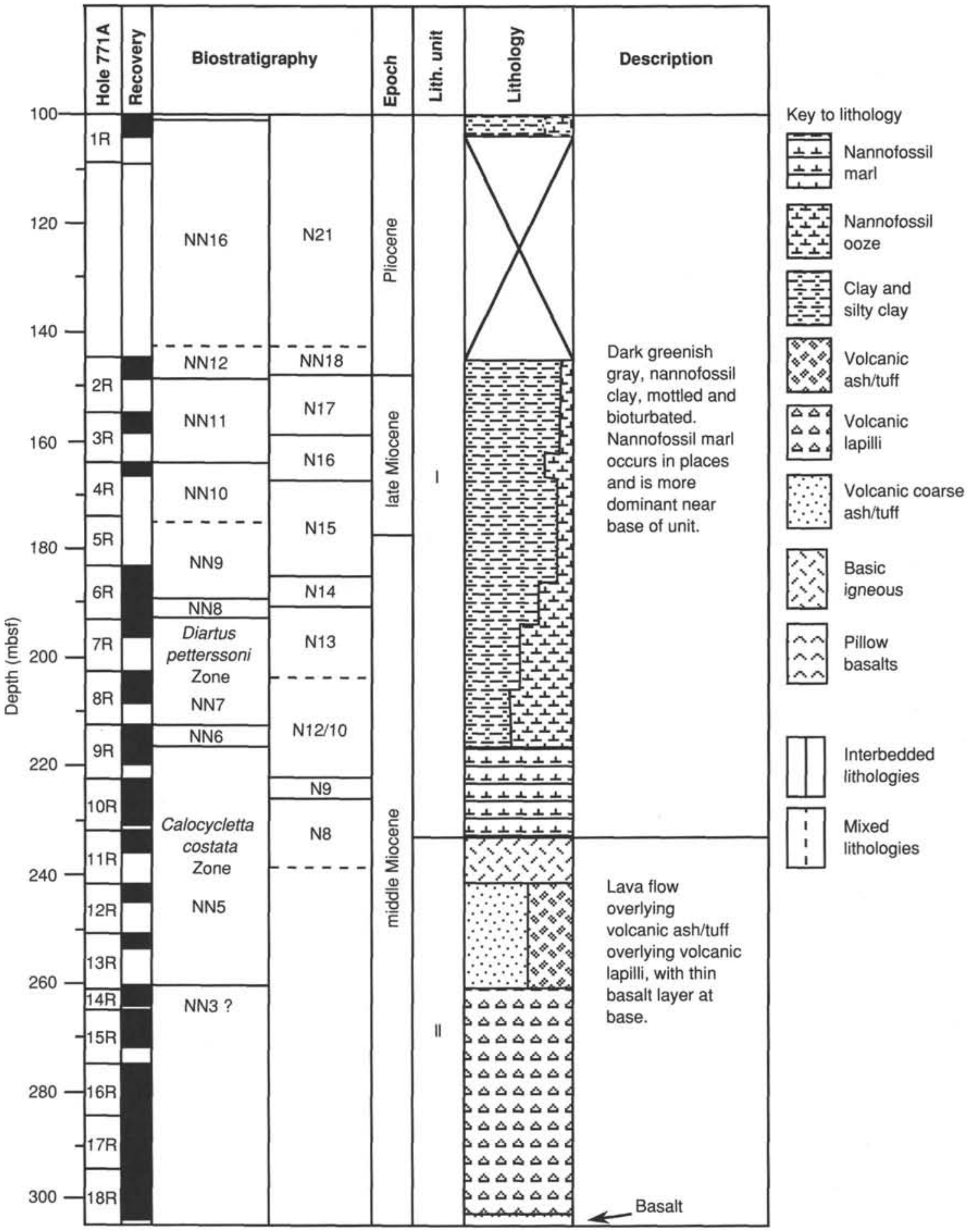

Figure 3. Graphic log of lithologic variations and units at Site 771.

The sediment is composed of clay, nannofossils, and very minor foraminifers, silt-size bioclasts, and plagioclase. The foraminifers and bioclasts (possibly fragments of foraminifers) increase in abundance downward in concert with the overall increase in carbonate content. Within this sequence there are irregular gradational alternations of carbonate-rich and carbonate-poor sediment on the scale of decimeters to several meters. Accompanying these smaller scale variations are changes in degree of preservation of nannofossils, with more severe dissolution effects evident in the more carbonate-poor intervals (see "Biostratigraphy" section, this chapter).

Thick laminae of grayish green silty clay interbedded in clay with nannofossils in Core 124-771A-3R may represent altered ash layers. Minor amounts of dispersed volcanic ash (glass, hornblende, plagioclase, and biotite) are present in the nannofossil clay and marl in the lower 30 m of Unit II. The basal 2 m consists of interbedded nannofossil marl, claystone and tuffaceous claystone, and very thin vitric tuff. The claystone and

Table 2. Lithologic units, Site 771.

Unit	Depth (mbsf)	Thickness (m)	Age
I	100–233.91	133.91	middle Miocene to late Pliocene
II	233.91–303.05	69.14	late early Miocene or older to early middle Miocene

tuffaceous claystone consist of clay, up to 25% volcanic glass, feldspar, biotite, and <10% nannofossils. The vitric tuff beds contain vesicular glass shards and opaque minerals. This sequence overlies the basalt that forms the top of Unit II, though the contact is not preserved in the cores because of severe drilling disturbance.

Unit II

Depth: 233.91–303.05 mbsf
Interval: Section 124-771A-11R at 41 cm through Core 124-771A-18R
Thickness: 69.14 m
Age: early middle to late early Miocene

Unit II is composed of volcaniclastic strata underlain and capped by basaltic lava flows. Thin-bedded coarse to fine tuffs occur below the upper basalt, but the predominant volcaniclastic rock is massive and structureless lapillistone.

Silty claystone interbedded with tuff in the upper part of Unit II is paleontologically dated as early middle Miocene. The top of the underlying lapillistone sequence (Section 124-771A-14R-1) was highly fractured during coring, but a single core piece contains an irregularly inclined contact between lapillistone and calcareous claystone with late early Miocene nannofossils. The claystone partially surrounds volcanic lapilli at the contact and contains some dispersed sand- to granule-size volcanic lithic clasts. On the basis of this relationship, we interpret the calcareous claystone as part of a sediment layer deposited on top of the lapillistone, rather than as a clast of older sedimentary rock included within it, and it therefore dates the top of the lapillistone as late early Miocene. The remainder of the lapillistone is nonfossiliferous.

Approximately 1.5 m of basalt was recovered at the top of Unit II (Sections 124-771A-11R-2 at 41 cm to 124-771A-12R-1 at 47 cm). The log of drilling-time variations through this interval suggests that the true thickness is not more than 3.0 m. The basalt is aphanitic, with few phenocrysts of plagioclase. The bulk of the basalt is sparsely vesicular, but the top and bottom portions are moderately vesicular, indicating that the basalt was formed as a single lava flow. Most of the vesicles are lined with thin coatings of bluish white silica or clay.

Coarse and fine tuff occur in medium to thin, normally graded beds below the upper basalt (from Sections 124-771A-12R-1 at 47 cm to 124-771A-14R-1 at 65 cm). The beds have sharp bases and may show a very thin zone of reverse grading at the base. Parallel lamination occurs in places in the coarse tuff beds. Very thin beds of dark green tuffaceous silty claystone occur interbedded with the tuff. The tuff is dominantly composed of volcanic glass with some plagioclase and lithic clasts.

Approximately 40 m of lapillistone forms most of the lower part of Unit II, from Sections 124-771A-14R-1 at 65 cm to 124-771A-18R-8 at 20 cm. The lapillistone is massive throughout, with no recognizable bedding surfaces or lamination. Variations in the average grain size and in the concentration of large (over 1 cm) clasts occur in Cores 124-771A-16R, -17R, and -18R. These variations define very thick fining-upward sequences in Cores 124-771A-16R and -18R.

The lapillistone is composed of lithic clasts of plagioclase-clinopyroxene phyric andesite, andesite with a brown glassy groundmass, and plagioclase-pyroxene andesitic basalt, with some pyroxene crystals. The larger lithic clasts, which are up to 11 cm in diameter at the base of the sequence, are generally highly vesicular and are subangular. Exotic nonvolcanic clasts (possibly siliceous metamorphic rock) occur in Core 124-771A-18R. Secondary pyrite and native copper grains are common.

At the base of the lapillistone sequence, 58 cm of basalt was recovered in Section 124-771A-18R-8. It is plagioclase-clinopyroxene-olivine phyric basalt and is vesicular in places. It may be either a large block of lava or a lava flow. Since the lava occurred at the bottom of the hole, the thickness is a minimum, and the underlying material was not seen.

Fractures and microfaults are common throughout Unit II. Microfaults in the upper tuff sequence appear to have formed prior to lithification of the tuffs. These microfaults have moderate apparent dips and normal dip-separation, and occur primarily in the dark silty claystone beds separating graded tuff beds. Some silty claystone beds have been extensively disrupted by sets of these microfaults and have undergone considerable bedding-parallel extension. Tuff has been injected downward along many of these microfaults prior to lithification, and in some cases the offset basal portion of a tuff bed may contain angular clasts derived from the adjacent silty claystone. Later fractures filled with a white silicate mineral are also present in the upper tuff sequence and the lapillistone.

Igneous Rock Petrology

Basaltic tuff and lapillistone and minor basaltic lavas compose the lower section of Hole 771A in the interval between 233.91 and 303.05 mbsf (Unit II described above). A petrographic and chemical study of representative samples from coarse tuff and lapillistone and from the upper and lower lavas was made after the cruise. We examined 14 samples under the microscope and selected 10 for chemical analysis. Major and trace elements were determined by X-ray fluorescence (XRF) analysis. These analyses were made after the cruise in the geochemical laboratory of the University of Udine, Italy, because of the lack of time on board. Detailed thin section descriptions of this material appear in the section following the barrel sheets, and the results of the chemical analyses appear in Table 3.

Petrography

One representative sample of coarse tuff (Sample 124-771A-13R-3, 102–105 cm), which constitutes the dominant lithology in the upper part of Unit II, consists mostly of rock fragments and minor proportions of crystals. The rock fragments are basalts with varied textures, but they are probably homogeneous in composition. The most abundant, composing about 40% of the rock volume, consist of glass completely altered to green or yellow-green smectite. The glass in some fragments includes microlites and crystallites of plagioclase and clinopyroxene. Less abundant fragments, composing about 25% of the rock, consist of hyalophyric and hypocrystalline porphyritic basalt and aphyric basalt.

Phenocrysts are dominantly plagioclase (labradorite), and more rarely of plagioclase and minor augite. The crystal component of the tuff is composed of plagioclase (An_{55-65}) and augite. Crystals of magnetite and of brownish green hornblende occur sparsely. Intergranular spaces amounting to about 20% of the rock volume are partly filled with zeolites and crystalline silica (probably cristobalite) and with some smectite.

Coarse tuff with lapilli interlayered with lapillistone from the middle and lower part of Unit II (Samples 124-771A-15R-4, 39–44 cm, and 124-771A-18R-3, 31–33 cm) are dominantly lithic as in the upper part, and are characterized by the occurrence of olivine as phenocrysts in the lithic clasts and as free crystals. Clasts consist mostly of basic glass altered to green, yellowish

Table 3. Major and trace element composition of the volcanic and volcaniclastic rocks at Site 771.

Core, section, interval (cm)	SiO_2	TiO_2	Al_2O_3	Fe_2O_3	MnO	MgO	CaO	Na_2O	K_2O	P_2O_5	Total	LOI	Mg#	Nb	Zr	Y	Sr	Rb	Ni	Cr	V	Ba
124-771A-																						
11R-3, 13–16	49.10	0.65	15.25	10.47	0.24	9.20	12.77	1.75	0.24	0.13	99.80	2.50	67	4	28	13	250	4	51	227	248	60
13R-2, 102–105	51.90	0.88	17.80	10.03	0.22	6.75	5.20	4.67	1.70	0.19	99.34	6.83	61	3	52	19	170	33	17	60	260	265
15R-3, 69–72	50.90	0.63	18.10	9.53	0.18	8.25	8.90	2.07	0.61	0.18	99.35	5.14	67	1	46	12	350	14	58	105	220	116
17R-2, 108–110	51.45	0.72	16.12	9.58	0.18	6.05	11.40	2.63	1.45	0.47	100.05	5.48	59	4	52	18	395	21	78	207	305	119
18R-3, 31–33	51.40	0.65	18.70	9.27	0.17	6.30	8.05	3.45	1.26	0.16	99.41	5.84	61	4	41	13	315	23	22	61	202	120
18R-3, 129–132	49.40	0.79	18.12	10.37	0.20	5.83	11.02	2.45	0.78	0.26	99.22	2.94	56	5	61	20	430	21	59	130	250	117
18R-7, 57–59	51.30	0.81	18.68	8.37	0.16	4.92	11.45	2.35	1.05	0.27	99.36	2.93	57	4	66	21	540	13	16	24	265	128
18R-7, 120–124	50.15	0.77	17.50	9.80	0.22	7.17	11.20	2.12	0.36	0.24	99.53	2.13	63	4	57	22	400	8	101	252	225	87
18R-7, 142–144	51.00	0.78	19.30	9.50	0.18	4.92	10.58	2.63	0.67	0.26	99.82	1.68	54	5	67	23	540	20	16	34	223	142
18R-8, 21–23	48.70	1.09	17.90	12.27	0.25	4.15	10.77	2.47	0.92	0.36	98.88	3.08	44	4	73	24	435	18	10	13	350	131

Note: Major element composition is given in oxide wt% and trace element contents in ppm element. LOI = loss on ignition.

green, or brownish green smectite and of hyalophyric basalt containing variable amounts of plagioclase phenocrysts or of plagioclase, augite, olivine, and magnetite.

A small proportion of the rock fragments consists of porphyritic basalt with phenocrysts of plagioclase, augite, and olivine and a texturally variable hypocrystalline groundmass showing an apparent oxidation of the glassy mesostasis. Pore spaces filled with clays and zeolites are less voluminous than in tuff from the upper part of Unit II. Isolated crystals are formed mostly of plagioclase occurring as aggregates of laths, and lesser amounts of olivine and clinopyroxene with granular inclusions of olivine. In all occurrences olivine is pseudomorphed by orange-green iddingsite.

Lapilli occurring in the lower part of Unit II include different basaltic rocks showing marked differences in texture, mostly in the proportion of phenocrysts and vesicles, as well as small differences in mineral assemblage. The following groups were distinguished petrographically:

1. Sparsely vesicular, moderately to highly phyric basalt (Samples 124-771A-15R-4, 39–44 cm, and 124-771A-18R-3, 129–132 cm) consisting of phenocrysts of plagioclase, augite, and olivine (altered to iddingsite) with a groundmass consisting of plagioclase, clinopyroxene, opaques, and glass. Glass is incipiently devitrified and oxidized. In Sample 124-771A-18R-3, 129–132 cm, the glass shows typical perlitic cracks along which alteration to smectite is developed.
2. Sparsely vesicular highly phyric basalt (Sample 124-771A-18R-7, 142–144 cm) similar in texture and essential mineralogy to the first group (above), but characterized by the occurrence of orthopyroxene as phenocrysts intergrown with olivine.
3. Highly vesicular, highly phyric basalt (Sample 124-771A-17R-2, 108–110 cm) composed of phenocrysts of plagioclase (bytownite-labradorite), augite, olivine, and magnetite and a hypocrystalline groundmass with hyalopilitic to pilotaxitic texture. Vesicles filled with clays, crystalline silica, and zeolites are present in high but variable proportions (7%–30%).
4. Highly vesicular, highly phyric basalt (Sample 124-771A-18R-7, 57–59 cm) similar in mineral assemblage and texture to basalts in the second group (above), but rich in vesicles (about 30% volume).

The 1.5-m-thick lava recovered at the top of Unit II is composed of fine-grained basalt (Sample 124-771A-11R-3, 13–16 cm) containing about 4% phenocrysts of augite in a groundmass of plagioclase, clinopyroxene, opaques (magnetite and ilmenite), and glass. Glass is completely altered to brown-green smectite, which also fills sparse vesicles; plagioclase shows incipient smectite alteration.

The basaltic rock recovered at the bottom of Hole 771A, in the lowermost 58 cm, was interpreted as a possible lava flow (Sample 124-771A-18R-8, 21–23 cm). It is moderately vesicular and contains a high proportion of plagioclase phenocrysts (about 15% of the rock volume) and minor proportions of olivine, clinopyroxene, and magnetite phenocrysts. Groundmass shows a hyalopilitic texture and consists of microlites of plagioclase, clinopyroxene, olivine, and opaques in partly altered and devitrified glass.

Chemistry

The chemical data reported in Table 3 reveals that the lavas composing the upper flow, the lapilli clasts in the volcaniclastic deposit, and the probable flow at the bottom of Unit II are basaltic, with rather variable composition in terms of major and trace element abundances. Downhole variations for selected major and trace elements are shown in Figure 4.

The upper basalt flow (Sample 124-771A-11R-3, 12–16 cm) shows a tholeiitic olivine-normative composition and low abundances of alkalis, TiO_2, and most incompatible trace elements. Its multi-element pattern, normalized to normal Mid-Ocean Ridge basalts (N-MORB) (Fig. 5) is similar to that of low-potassium tholeiites.

Basalts occurring as lapilli in lapillistone and coarse tuff from the middle and lower part of Unit II show moderately variable composition, and are distinguished from the basalt of the upper flow by higher SiO_2, Al_2O_3, and alkali abundances. The K_2O contents (if not strongly affected by secondary processes) seem to indicate a tholeiitic (low-Ti) to calc-alkaline serial character. This is also suggested by N-MORB normalized minor and trace element patterns (Fig. 5).

The basaltic flow at the bottom of Hole 771A is distinct chemically from the other basalts mostly because of the higher total Fe_2O_3 and lower MgO content. The amount of K_2O relative to silica seems to indicate a calc-alkaline character.

Chemical data on the three analyzed tuff samples, though not representative of a magma composition, support their origin from basaltic magmas similar to those represented among the lapilli. The basaltic nature of the volcanic detritus is confirmed particularly for those rocks rich in glass with a composition and relation to clasts poor in glass that could not be ascertained by petrographical features alone.

Depositional Environment and Processes

Site 771 is located on the Cagayan Ridge, at a present water depth of about 2859 mbsl; it is the shallowest of the three sites drilled in the Sulu Sea on Leg 124. Two major phases of sedimentation were recognized in the stratigraphic sequence recovered at Site 771, corresponding to the two lithologic units into which the section has been divided. The earlier phase (early middle Miocene to late early Miocene or older) produced the volcaniclastic strata with intercalated basalt flows of Unit II. The succeeding phase (middle Miocene to late Pliocene) resulted in the accumulation of mixed hemipelagic clay and pelagic carbonate sediments of Unit I.

The volcanic rocks and associated lavas composing Unit II of Site 771 consist of basalts similar in chemical and petro-

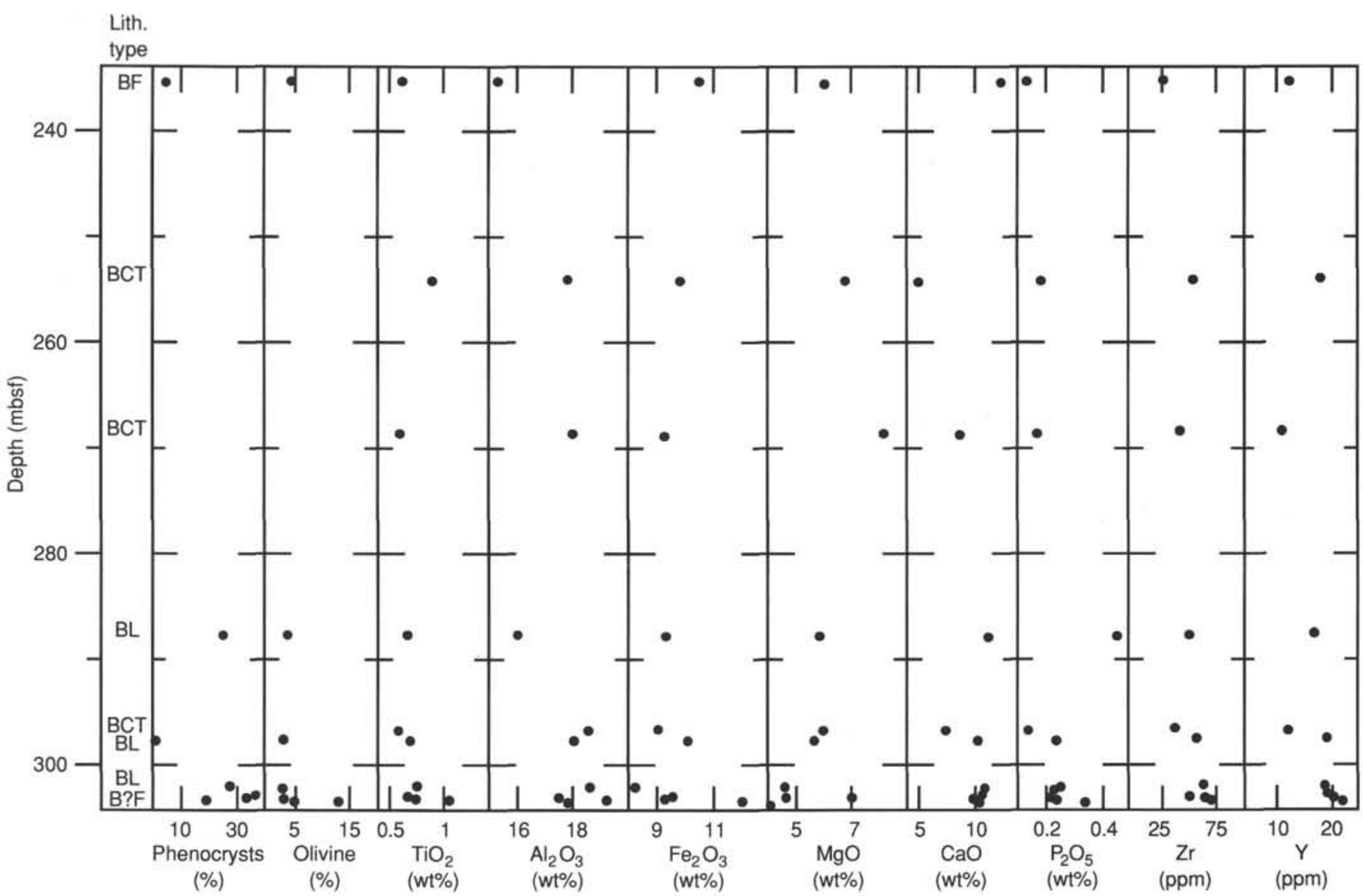

Figure 4. Downhole variations of selected major and trace elements in Unit II of Site 771. The lithologic types shown in the figure include basalt flow (BF), basaltic lapilli (BL), and basaltic coarse tuff (BCT).

graphical features to basalts of low-K tholeiitic and calc-alkaline type. The presence of hypersthene and magnetite in the phenocryst assemblage as well as the inferred crystallization sequence support this interpretation.

A brief comparison of the petrographical and chemical features compared with those of the igneous rocks recovered at Sites 769 and 771 indicates that both suites of rocks derive from petrologically similar magmas erupted in an island arc. At Site 771 less fractionated products of basaltic composition occur, whereas at Site 769 a wider spectrum of fractionated products ranging from basalt to andesite are represented.

The intercalation of flows and pyroclastic deposits suggests close proximity to the vent (or vents). The upper graded tuff beds are clearly turbidites intercalated with marine silty claystone with nannofossils. The thin basalt flow at the top of the unit overlies the ash turbidites and is succeeded by fine-grained hemipelagic/pelagic claystone and marlstone, indicating submarine emplacement of the flow. The depositional setting of the massive lapillistone in the lower part of Unit II is more difficult to assess. It must have accumulated rapidly, in view of the lack of interbedded sediment. We regard the lapillistone as either a near-vent fallout deposit from pyroclastic eruptions, or as a deposit from subaerial or submarine mass flows of pyroclastic material down the slopes of the volcano. The superposition of ash turbidites above massive lapillistone reflects waning volcanic activity (interrupted by the capping basalt flow), and may also signify a concurrent deepening of the site.

The boundary between Units I and II represents a rapid transition in early middle Miocene time from volcaniclastic sedimentation to hemipelagic/pelagic sedimentation. Only minor amounts of disseminated ash are found in the basal strata of Unit I, and these decrease to trace amounts within a few meters above the base. For the remainder of middle Miocene through early Pliocene time, concurrent deposition of hemipelagic clay and pelagic biogenic carbonate sediment characterized the site. This record of sedimentation indicates that Site 771 has remained above the CCD for much of Neogene time. However, dissolution effects are evident in nannofossil and foraminifer assemblages (see "Biostratigraphy" section, this chapter), implying that the site was deeper than the calcite lysocline for much of this interval. The upward decrease in carbonate content through Unit I may have been the result of increasing rates of dissolution caused by the gradual subsidence of the Cagayan Ridge through middle Miocene and Pliocene time. This conjecture, however, cannot be substantiated in the absence of independent control on the Neogene history of the CCD in the Sulu Sea.

Comparison of Sites 769 and 771

Sites 769 and 771 are located on the Cagayan Ridge, which forms the northwestern flank of the deep basin of the eastern Sulu Sea. Drilling at each site ended in coarse volcaniclastic strata of andesitic to basaltic composition, which are early middle Miocene to late early Miocene or older. During this interval the Cagayan Ridge appears to have been the site of active arc volcanism. The volcaniclastic rocks at both sites are significantly more mafic than the roughly coeval dacitic to rhyolitic pyroclastic flows encountered at Site 768 in the deep Sulu Sea basin.

Volcanism on Cagayan Ridge ceased rather abruptly, and the overlying middle Miocene and younger sequence at both sites consists of hemipelagic to pelagic sediment that is much re-

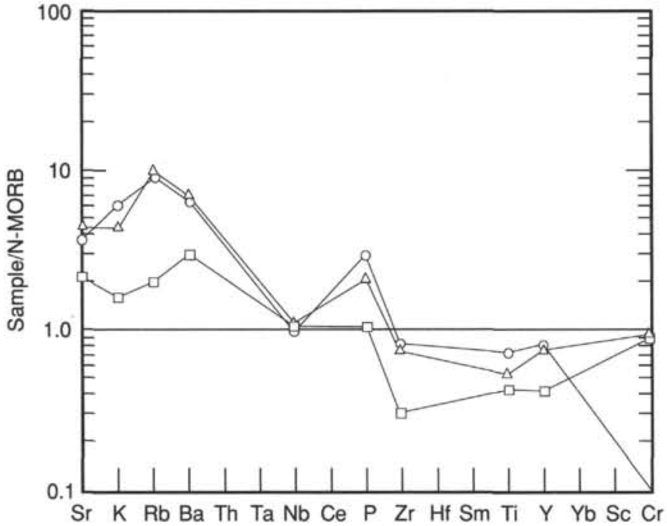

Figure 5. N-MORB normalized minor and trace element patterns of selected samples of igneous rocks, Site 771. Normalizing values for N-MORB are from Pearce (1982). Square = Sample 124-771A-11R-3, 13–16 cm; triangle = Sample 124-771A-18R-7, 142–144 cm; and circle = Sample 124-771A-18R-8, 21–23 cm.

duced in thickness relative to coeval sediment in the deep Sulu Sea. Site 771 is currently about 950 m shallower than Site 769, and this depth difference has had a major control on later Neogene sedimentation at the two sites. Through later middle Miocene to early Miocene time, the CCD was deeper than Site 771 but shallower than Site 769, resulting in the near absence of pelagic carbonate sediment at the latter site, in contrast to mixed clay and pelagic carbonate deposition at Site 771.

Despite the additional input of carbonate sediment at Site 771, the thickness of the middle Miocene to Pliocene section at both sites is roughly comparable, suggesting that the absence of carbonate sedimentation at Site 769 was counteracted by a somewhat higher rate of hemipelagic clay deposition. At Site 769 a major change in sedimentation occurred in late Pliocene time, with the appearance of nannofossil marl that dominates the uppermost Pliocene to Pleistocene section. We have interpreted this change as indicating a drop in the CCD within the Sulu Sea during late Pliocene time (see "Lithostratigraphy" section, "Site 769" chapter, this volume). The effects of this change at Site 771 cannot be assessed, since the uppermost Pliocene to Pleistocene section was not cored.

BIOSTRATIGRAPHY

Summary

Site 771, drilled at 2859 mbsl on the Cagayan Ridge, was spot cored in the upper part to about 145 mbsf. After that, it was drilled continuously with rather poor recovery.

The continuously drilled and complete sedimentary sequence, overlying the volcanic basement at 233.9 mbsf, ranges in age from early Pliocene to late early–early middle Miocene (NN5, N8, *Calocycletta costata* Zone). Core 124-771A-1R, taken at 100 mbsf, belongs to the upper Pliocene (NN16, N21).

This site has been, throughout the time represented by the sediments, above the CCD. As a result, biostratigraphic control is good (Fig. 3). The sediments are generally rich in calcareous nannofossils and planktonic foraminifers. Changes in abundance and preservation of these fossil groups indicate fluctuations in the strength of dissolution. It is possible to observe a certain cyclicity within the sedimentary sequence because of the varying carbonate content.

Moderately to poorly preserved radiolarians are present in Core 124-771A-7R (*Diartus petterssoni* Zone; preserved by pyritization) and in Cores 124-771A-10R and -11R (*Calocycletta costata* Zone) directly above the basement. The presence of calcareous and siliceous fossils within the lowermost part of the sequence allowed better age control for the cessation of the volcanic activity of the Cagayan Ridge than at the other sites drilled in the Sulu Sea. Nannofossils recovered from within the pyroclastics (Core 124-771A-12R to Section 124-771A-14R-1) belong to Zone NN5, similar to that found above. Sample 124-771A-14R-1, 62–63 cm, belongs to the lower Miocene (probably upper part of Zone NN3).

Nannofossils

The sediments recovered at Site 771 range in age from late Pliocene to early middle Miocene. Nannofossils are common to abundant and better preserved at this site. All middle and late Miocene nannofossil zones were identified with the markers given by Martini (1971).

Core 124-771A-1R (100 mbsf) is of late Pliocene age. *Discoaster surculus* was found in Section 124-771A-1R-1 and thus is assigned to *D. surculus* Zone (NN16).

Core 124-771A-2R was taken at 144.7 mbsf. Sediments from the top to Sample 124-771A-2R-2, 19–20 cm, are assigned to early Pliocene Zone NN12. The upper Miocene (Zone NN11) was determined from Sample 124-771A-2R-2, 49–50 cm, to Sample 124-771A-4R-1, 40–41 cm. The interval from Sample 124-771A-4R-1, 108 cm, to Sample 124-771A-4R-CC is assigned to Zone NN10. Zone NN9 is determined from Samples 124-771A-5R-1, 7–8 cm, to 124-771A-6R-7, 39–40 cm (193.0 mbsf), by the presence of *D. hamatus*.

The next datum level is the first occurrence (FO) of *Catinaster coalitus*, which marks the base of Zone NN8 in Sample 124-771A-7R-2, 40–41 cm (195.1 mbsf). The lowest occurrence of *Discoaster kugleri* was encountered in Sample 124-771A-9R-1, 75–76 cm (213.3 mbsf), and defines the base of Zone NN7. Sediments from this level to Sample 124-771A-9R-3, 50–51 cm, are assigned to Zone NN6. *Sphenolithus heteromorphus*, the highest occurrence of which is used to divide Zones NN6 and NN5, was found in Sample 124-771A-9R-3, 75–76 cm (216.3 mbsf). Nannoplankton Zone NN5 was also recognized in the sediments included within the pyroclastics (Core 124-771A-12R to Section 124-771A-14R-1). Sample 124-771A-14R-1, 62–63 cm, taken from a marl within the lapillistone, belongs to the lower Miocene (probably upper part of Zone NN3), as inferred from the presence of very rare specimens of *Sphenolithus belemnos* and *Sphenolithus heteromorphus*.

Foraminifers

Sediments in Cores 124-771A-1R to -11R are mostly carbonate rich. Foraminifers are present throughout the section. Most samples show signs of dissolution, varying from a little to severe fragmentation. Changes in preservation indicate fluctuations in the depth of the CCD. Foraminifer ages are summarized in Figure 3.

Core 124-771A-1R is mostly poor in carbonate. Two thin levels that are more carbonate rich yield moderately well-preserved foraminifer faunas. Right-coiling *Globorotalia menardii* is present in samples from those levels, whereas *Globoquadrina altispira* is absent, indicating a late Pliocene age (N21).

Cores 124-771A-2R through -11R were taken in upper and middle Miocene sediments. Most samples show signs of dissolution, and *Sphaeroidinellopsis* spp. are the most common planktonic foraminifers. Core-catcher samples, and additional samples from selected cores, allow recognition of most of the foraminifer Zones N18 through N8. The FO of *Globorotalia tumida* in Sample 124-771A-2R-1, 16–18 cm, marks the lower boundary of Zone N18. The presence of right-coiling *Neogloboquadrina acostaensis* in Sample 124-771A-2R-CC indicates that this sample belongs to the upper part of Zone N17. Sample 124-771A-3R-CC still belongs to Zone N17, whereas Sample 124-771A-4R-CC gives Zone N16 as an age.

We recognized Zone N14 in Samples 124-771A-6R-4, 59–61 cm, and 124-771A-6R-6, 55–57 cm, by the co-occurrence of *Globigerina nepenthes* and *Globorotalia siakensis*. Representatives of the *Globorotalia peripheroacuta–Globorotalia fohsi* lineage are present in Samples 124-771A-8R-4, 20–22 cm, through 124-771A-9R-CC, giving a Zone N12 through N10 age to this part of the section. However, *G. fohsi* s.l. specimens are very rare and do not allow further subdivision.

The top of Zone N8 should be recognized by the FO of *Orbulina suturalis*. However, *Orbulina* spp. are rare throughout most of the Miocene sediments, probably as a result of selective dissolution. The top of Zone N8 is tentatively placed between Samples 124-771A-10R-2, 39–41 cm, and 124-771A-10R-3, 16–18 cm. Sections 124-771A-10R-3 through 124-771A-10R-CC yield faunas that are better preserved than those from overlying sediments, and they contain common *Globigerinoides sicanus, Praeorbulina glomerosa*, and *Praeorbulina transitoria*. The absence of *Orbulina* spp. in these samples is thought to be biostratigraphic rather than the result of preferential dissolution. *Globorotalia sicanus* is also found in Sample 124-771A-11R-2, 18–21 cm, giving a lower middle Miocene age (Zone N8) to the sediments directly overlying the pyroclastic deposits.

Diatoms

Diatoms are absent from all sediments collected at Site 771, with the exception of pyritized *Ethmodiscus* sp. fragments seen in radiolarian preparations (>44 μm) of upper middle Miocene sediments (Sample 124-771A-7R-CC).

Radiolarians

Radiolarians are absent in samples from Cores 124-771A-1R and -2R. The core catcher of Core 124-771A-3R contains trace amounts of pyritized radiolarian fragments, but no whole specimens were seen. Samples from Cores 124-771A-4R through -6R are barren of radiolarian remains.

Sample 124-771A-7R-CC (202.9 mbsf) contains an assemblage of rare pyritized radiolarians of the *Diartus petterssoni* Zone, late middle Miocene in age. The assemblage includes *Didymocyrtis laticonus* and *Stichocorys delmontensis* as well as *D. petterssoni*. This corresponds with an identical pyritized radiolarian assemblage seen at Site 769, suggesting widespread stratification of the water column in the Sulu Sea during this time.

Sample 124-771A-8R-CC contains rare and poorly preserved radiolarians of indeterminate age. Samples from Core 124-771A-9R are barren or nearly so, yielding no radiolarian age control. In contrast, radiolarians are present in great abundance in samples from Core 124-771A-10R, but preservation is poor. Samples from 124-771A-10R-3, 73–75 cm (226.3 mbsf), to the core catcher (232.0 mbsf) contain radiolarians of the *Calocycletta costata* Zone (upper lower Miocene to lower middle Miocene). These include *C. costata, Stichocorys wolffii, S. delmontensis, Didymocyrtis violina, Cyrtocapsella cornuta*, and *Calocycletta virginis*.

Samples from Core 124-771A-11R contain radiolarians of the same zone as described above, but preservation is generally somewhat better in these samples. Sample 124-771A-11R-1, 149–150 cm, contains *Cyrtocapsella tetrapera* and abundant *Zygocircus* sp. in addition to those listed above; and Sample 124-771A-11R-2, 35–37 cm, contains the *simplex* form of *Dorcadospyris forcipata*. Volcanic sediments underlying this level are barren of radiolarians.

The oldest age obtained by radiolarians at Site 771 is late early to early middle Miocene, *C. costata* Zone. This corresponds well with ages determined from other Sulu Sea sites (768 and 769); although at these sites, it is not yet clear if sediments overlying basement are of the *C. costata* Zone or the *S. wolffii* Zone because of the poor radiolarian preservation in those sediments.

Ichthyoliths

At Site 771, ichthyoliths are very rare throughout the section. Core-catcher samples yielded only a few unbroken specimens, but no age-diagnostic forms. No attempt at further analysis was made.

PALEOMAGNETICS

The reduced drilling program at Site 771 allowed only RCB coring, and therefore cube and minicore samples were taken for paleomagnetic studies. The highly disturbed RCB cores, however, were not ideal for paleomagnetic work and have produced poor data. Figure 6 shows the paleomagnetic data (at a 20-mT alternating-field [AF] demagnetization level) for Site 771 measured on board the *JOIDES Resolution*.

Sediments

The absolute inclinations for sediment cores had scattered values that ranged from 2.8° to 76.2°. Core 124-771A-6R (183.6–193.2 mbsf) had especially inconsistent high inclinations averaged at 58.4°. This high inclination, which corresponds to a paleolatitude of 39.1°, cannot be attributed to movement of plate. Since the declinations also clustered near each other (Fig. 6), a strong overprint not removable by 20-mT AF demagnetization was suspected for Core 124-771A-6R. Splitting by wire for this rather hard core is a possible cause of the magnetic overprint.

The average inclination for the sediments (excluding Core 124-771A-6R) was 29.7°, which corresponds to a site paleolatitude of 15.6°, and no consistent changing trend could be found. The magnetization of the sediments was found to be weak but stable. Shipboard demagnetization experiments indicated that some samples require higher AF fields to reveal the primary components.

Coarse Tuff and Lapillistone

Tuff material appeared in Core 124-771A-11R at a depth of 233.9 mbsf. The tuffs had very unstable remanent magnetization with wide ranges of direction, magnetization intensity, and coercivity spectra. The inclinations (Fig. 6) were very scattered and so were the intensities. Figure 7 shows a high coercivity sample that essentially was not demagnetized by AF fields up to 20 mT. Figure 8 shows another sample that requires more demagnetization. A sample taken from a basaltic block was measured and found to have very different directions relative to nearby tuffs, indicating a low temperature during deposition. Our tentative conclusion is that these chaotic coarse-grained tuffs are simply not good material for recording the ancient

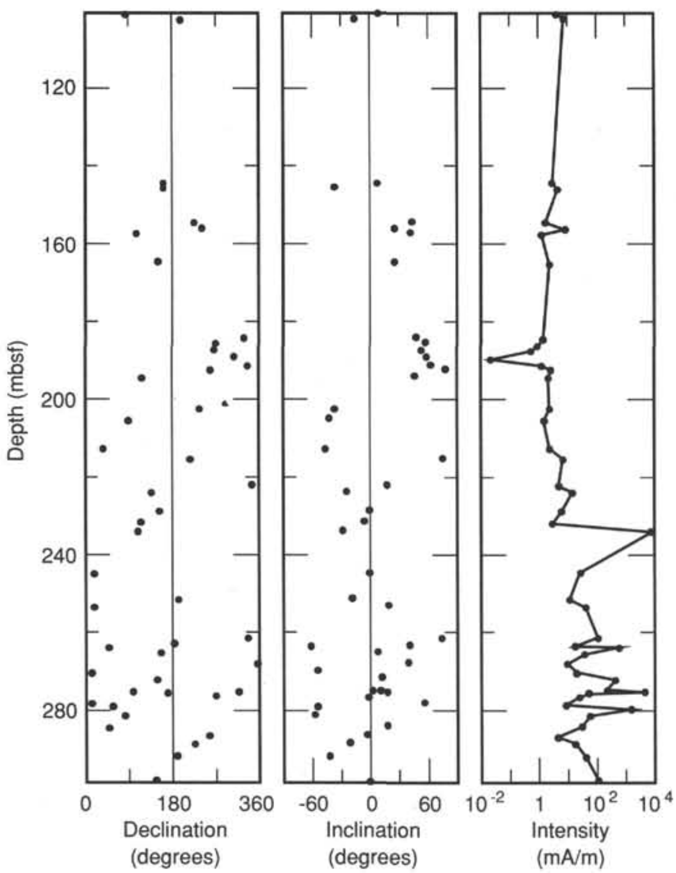

Figure 6. Magnetostratigraphic plot of declination, inclination, and intensity for Site 771. The data shown are at the 20-mT alternating-field demagnetization level. Tuff material starts at a depth of ~240 mbsf.

earth's magnetic field. More intensive shore-based demagnetization experiments are needed to verify this tentative conclusion.

Magnetic Susceptibility

Magnetic susceptibility plots for Site 771 are shown in Figure 9. Site 771 was not continuously cored. Core 124-771A-1R recovered sediments from 100 to 103.17 mbsf. Cores 124-771A-2R through -18R were drilled from 144.7 mbsf to a total depth (TD) of 304.1 mbsf. Whole-core susceptibility data were collected from Cores 124-771A-1R through -13R. Within the interval measured, two major susceptibility units are identified on the basis of the character of the susceptibility curve.

Susceptibility Unit 1 extends from 100 to 233.9 mbsf and occurs entirely within hemipelagic sediments. The susceptibility curve exhibits low variability, with average values between 60 and 120 $\times 10^{-6}$ cgs.

Susceptibility Unit 2 extends from 239.5 mbsf to at least the base of Core 124-771A-13R (261.0 mbsf). Tuffs and possible volcanic flows dominate this interval, with susceptibility values characteristically high within these lithologies. Very high susceptibility values (up to 1760 $\times 10^{-6}$ cgs) occur at the top of this unit in response to a probable volcanic flow. In the underlying pyroclastic sediments, susceptibility values average 400–500 $\times 10^{-6}$ cgs and exhibit extreme variability. Absolute values are not meaningful in these cores since the cores do not fill the liner. Many areas of these cores are filled with rubble, and susceptibility values are not comparable with other areas within the same section of core.

Whole-core susceptibility measurements were discontinued below Core 124-771A-13R for the above reasons. These cores probably can be included with Susceptibility Unit 2 since their lithologies are comparable with those of the measured cores.

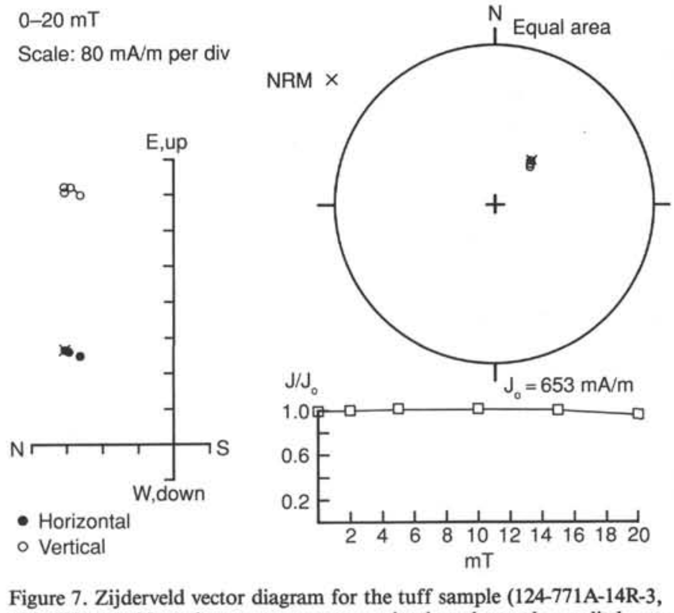

Figure 7. Zijderveld vector diagram for the tuff sample (124-771A-14R-3, 120–122 cm). Note that remanent magnetization changed very little up to 20 mT because of the high coercivity.

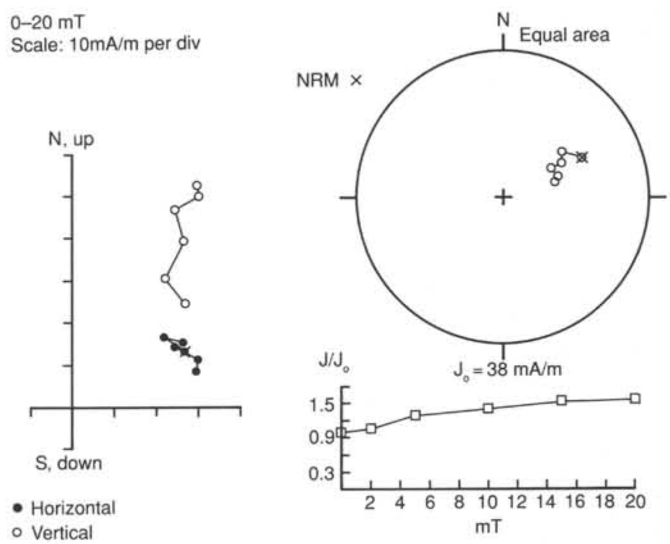

Figure 8. Zijderveld vector diagram for the tuff sample (124-771A-16R-6, 48–50 cm). The sample is highly unstable, as indicated by the increasing intensity and changing directions upon alternating-field demagnetization up to 20 mT.

SEDIMENT ACCUMULATION RATES

Sediment accumulation rates were determined at Site 771 with the use of biostratigraphic data. Only one core was taken (at 100.0 mbsf) in the upper 144.7 m of this hole. Below 144.7 mbsf, RCB coring was continuous; however, core recovery was variable, which decreased the accuracy of several biostratigraphic zone boundaries. Magnetostratigraphic studies were not undertaken at this site because of the discontinuous coring operation and the disturbed nature of the cores.

The time scale of Berggren et al. (1985) was used for age assignment to biostratigraphic zones. Calcareous nannoplankton zones are described in Martini (1971) and radiolarian zones are

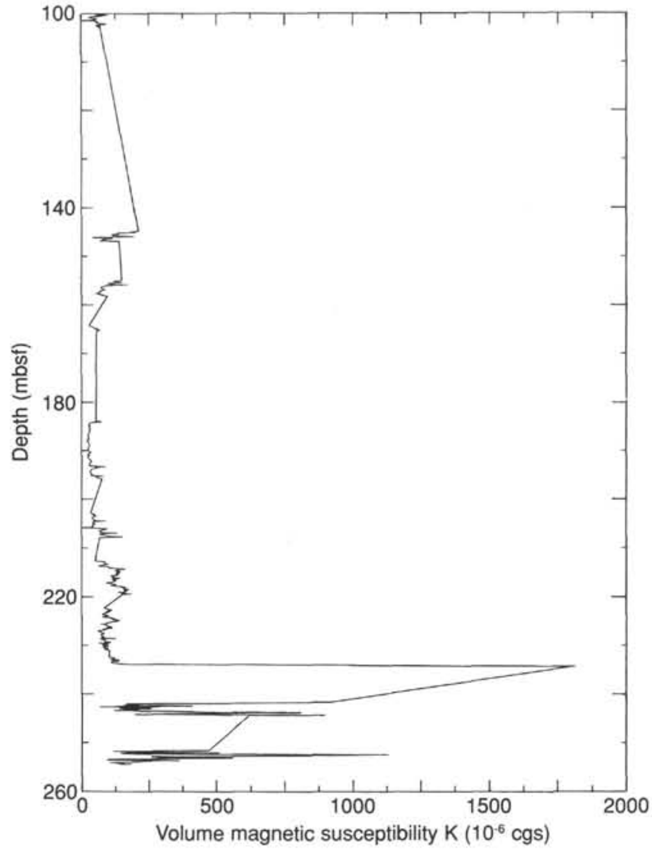

Figure 9. Magnetic susceptibility data, Site 771.

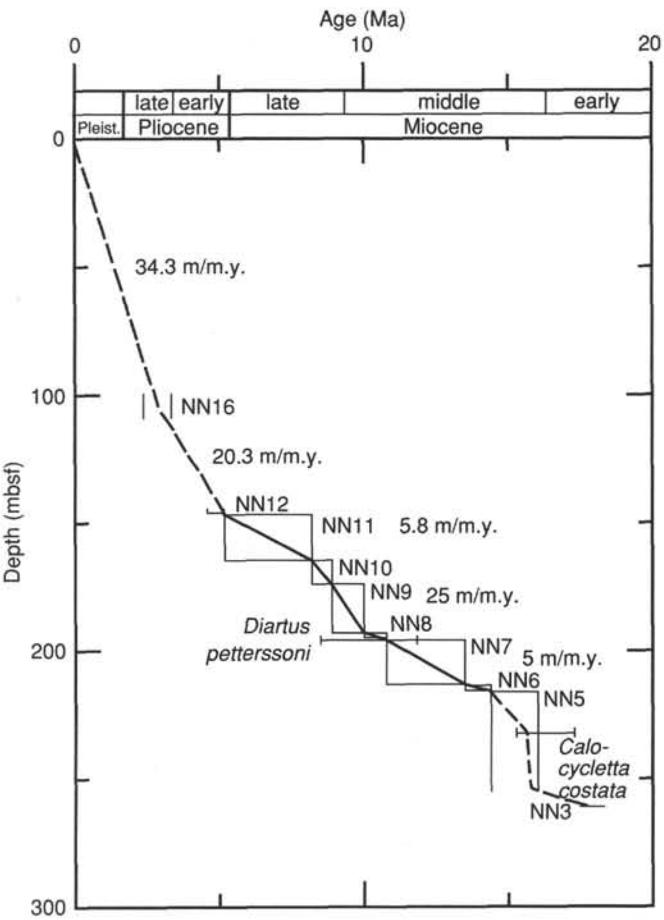

Figure 10. Sedimentation rates calculated from biostratigraphic data, Site 771.

defined by Riedel and Sanfilippo (1978). Sedimentation rates calculated from biostratigraphic markers are shown in Figure 10. Ages, intervals, and sedimentation rates of individual biozones identified are found in Table 4.

In Core 124-771A-1R nannofossil Zone NN16 and foraminifer Zone N21 were identified. Core 124-771A-2R includes the boundary between nannofossil Zones NN12 and NN11 and foraminifer Zones N18 and N17. These biomarkers are the only sedimentation rate controls for the upper 150 m of Hole 771A. Recognizing that the biostratigraphic control is very poor, we can calculate loosely constrained sedimentation rates of 34.3 m/m.y. and 20.3 m/m.y. for the intervals from 0 to 100.43 mbsf and from 100.43 to 146.4 mbsf, respectively.

Sediments in the continuously cored interval, down to the volcanic tuffs in Core 124-771A-11R, contained well-preserved fossil assemblages. Biomarkers were located with the help of nannofossils, foraminifers, and radiolarians. Nannofossil zones are well constrained, and ages determined by nannofossil zonations are supported by foraminifer and radiolarian data.

Sedimentation rates can be divided into several linear segments. Throughout Zone NN11 (147.5–164.6 mbsf), sedimentation rates average 5.8 m/m.y. From the top of Zone NN10 (164.6 mbsf) to the base of Zone NN9 (193.0 mbsf), sedimentation rates average 25 m/m.y. Sedimentation rates decrease from the previous interval to an average of 5 m/m.y. within the interval from Zones NN8 (193.0 mbsf) to NN6 (216.3 mbsf).

The base of Zone NN5 was not observed in Hole 771A, but sedimentation rates within this nannofossil zone are constrained by foraminifer and radiolarian zones. From the top of nannofossil Zone NN5 (216.3 mbsf) to the base of foraminifer Zone N9 (224.2 mbsf), the sedimentation rate averages 10 m/m.y. Below the base of foraminifer Zone N9, sedimentation rates are not well constrained but must be >38 m/m.y. because nannofossil Zone NN5 is observed down to Core 124-771A-13R (254.8 mbsf). Nannofossil Zone NN3 was observed in sediment just

Table 4. Ages, depths, and sedimentation rates for individual biozones identified at Site 771.

Biozone	Age (m.y.)	Depth (mbsf)	Sed. rate (m/m.y.)
NN16	2.45–3.4	100.0–?	
NN12	4.6–5.2	?–147.5	
NN11	5.2–8.2	147.5–164.6	5.8
NN10	8.2–8.9	164.6–174.6	12.3
NN9	8.9–10.0	174.6–193.0	17.6
NN8	10.0–10.8	193.0–195.1	2.8
NN7	10.8–13.5	195.1–213.3	6.6
NN6	13.5–14.4	213.3–216.3	3.3
NN5	14.4–16.0	216.3–?	
NN3		261.6	
D. petterssoni	8.5–11.8	195.9	
C. costata	15.3–17.3	231.4–234.0	
N21	1.9–3.0	103.2	
N17	5.3–7.2	147.3–158.4	
N15	10.2–10.4	165.7–185.8	
N14	10.4–11.3	188.7	
N13	11.3–11.6	193.2–195.9	9.0
N12/N11	11.6–13.9	208.1	
N10	13.9–15.0	219.7	
N9	15.0–15.2	222.5–224.2	9.0
N8	15.2–16.6	225.5–231.4	4.0

above the basement (261.6 mbsf), suggesting a large decrease in sedimentation rates to <4 m/m.y.

ORGANIC GEOCHEMISTRY

Scientific purposes of Leg 124 shipboard organic geochemistry studies were previously outlined in the "Organic Geochemistry" section of the Site 767 chapter (this volume). The following summarizes the preliminary shipboard results of Site 771 (Sulu Sea).

Samples

We collected 10 sediment samples from Site 771. All sediments were analyzed for the composition of light hydrocarbons with headspace analyses. Details of the analytical methods used are given in the "Explanatory Notes" chapter (this volume).

Results and Discussion

Background concentrations of methane are observed in all headspace gas samples (Table 5), indicating that no biogenic or thermogenic gas production occurs in the sediments of Site 771.

PHYSICAL PROPERTIES

Introduction

The physical properties determined from the materials recovered at Site 771 include index properties (i.e., wet-bulk density, grain density, porosity, water content, and void ratio), as determined from measurements by pycnometer and balance, and compressional wave velocity measured on discrete samples with the Hamilton Frame apparatus. Testing procedures are described in the "Explanatory Notes" chapter (this volume). No thermal conductivity or shear strength measurements were made at Site 771.

The lithologic units used in this section are those described in the "Lithostratigraphy" section (this chapter). Only spot coring was performed in the upper portion of the sediment column of Site 771. Because of the limited amount of data, our interpretation of physical property variations and depths of property boundaries is only approximate. Velocities and index properties were measured on all cores taken at Site 771. The values of the various physical properties measured are listed in Tables 6 and 7, and the variations of these properties with depth are illustrated in Figures 11 and 12.

Results

Index Properties

Figure 11 shows a pattern of smoothly increasing wet-bulk density with depth through the sampled portion of Unit I, a calcareous clay/claystone sequence. Wet-bulk density ranges from 1.4 to 1.5 g/cm^3 at 100 mbsf, increases to 1.6 g/cm^3, and reaches ~1.9 g/cm^3 at the base of the unit (233.91 mbsf). Wet-bulk density in Unit II, a volcaniclastic unit, shows an increase with depth in the upper part of the unit from ~1.8 g/cm^3 to 2.21 g/cm^3 at 265.78 mbsf. The wet-bulk density of the volcaniclastic unit is 2.20 g/cm^3 at the base of the unit, but there is a slight decreasing trend in wet-bulk density toward the base of the drilled sequence.

Table 5. Methane concentration of headspace gas samples (Carle GC) from sediments of Site 771.

Core, section, interval (cm)	Depth (mbsf)	Methane (ppm)
124-771A-		
1R-2, 0–3	101.50	2.40
2R-2, 0–3	146.00	3.00
3R-3, 0–3	157.60	2.80
4R-1, 137–140	165.60	2.30
6R-1, 147–150	185.10	2.50
7R-2, 0–3	194.70	2.40
8R-3, 0–3	205.90	2.30
9R-3, 0–3	215.60	2.20
10R-2, 0–3	223.80	2.60
11R-1, 137–140	233.40	2.60

Grain density at Site 771 is nearly constant throughout Unit I at a value centered between 2.65 and 2.70 g/cm^3, but the scatter of the profile is large (Fig. 11). Grain density decreases to between 2.65 and 2.35 g/cm^3 in the volcaniclastic rocks of Unit II.

The material drilled at Site 771 shows a pattern of smoothly decreasing porosity with depth in the sediment section, suggesting compaction caused by gravitational loading through continued deposition (Fig. 11). The porosity of the sediment is 81% at 100 mbsf and decreases to approximately 60% at the base of Unit I. The porosity of the basal volcaniclastic rocks varies between 15% and 40%. There appears to be a trend toward increasing porosity at the base of the hole.

The plot of water content vs. depth (Fig. 11) shows a decrease downward in the sediment column, with values from 100% to 150% in Core 124-771A-1R (100.2–102.5 mbsf), decreasing to levels between 40% and 50% at the base of Unit I. The water content of the volcaniclastic rocks is uniform at values from 10% to 25%, but there is a trend toward increasing values in the bottom 15–20 m of the sampled interval.

Figure 11 also shows that the void ratio (the ratio of voids to solids) follows a nearly coincident pattern as the water content. This is to be expected for sediment that is completely saturated with fluid.

Velocity

The compressional wave velocity values of discrete samples from Hole 771A are presented in Table 7 and plotted in Figure 12. The plot of velocity shows only a very small increase in velocity with depth in the sampled section of Unit I. The velocity values fall within a narrow range near 1.55 km/s, with no increase near the basement interface. The contact between the sediment and the underlying volcaniclastic unit is reflected in an abrupt increase in velocity from 1.55 km/s in the sediments to ~2.5 km/s. Velocity values in Unit II go as high as 4.0 km/s.

Conclusions

In general, all of the physical properties measured at Site 771 displayed the expected depth-dependent variations. Wet-bulk density increases with depth, almost certainly a result of compaction caused by gravitational loading. This observation is corroborated by the porosity, water content, and void ratio measurements, which all decrease with depth. However, there may be a tendency for wet-bulk density to decrease in the last 15–20 m of the drilled interval, with attendant increases in water content and porosity (with grain density remaining constant). This pattern is similar to that observed in the lowermost intervals at Site 769, also located on Cagayan Ridge.

Grain density values were nearly constant throughout the calcareous claystone unit, but they decreased in the underlying volcaniclastic unit. This probably reflects the abundance of low-density components in the volcaniclastic rocks, such as volcanic glass. Compressional wave velocity provides the most obvious indicator of the contact between the sediment and volcaniclastic rocks. The pyroclastic unit has a much higher velocity than the sediments, and the interface between the two is extremely sharp. These attributes of the contact give rise to the extremely strong and continuous reflection event seen on the seismic reflection profiles across Site 771.

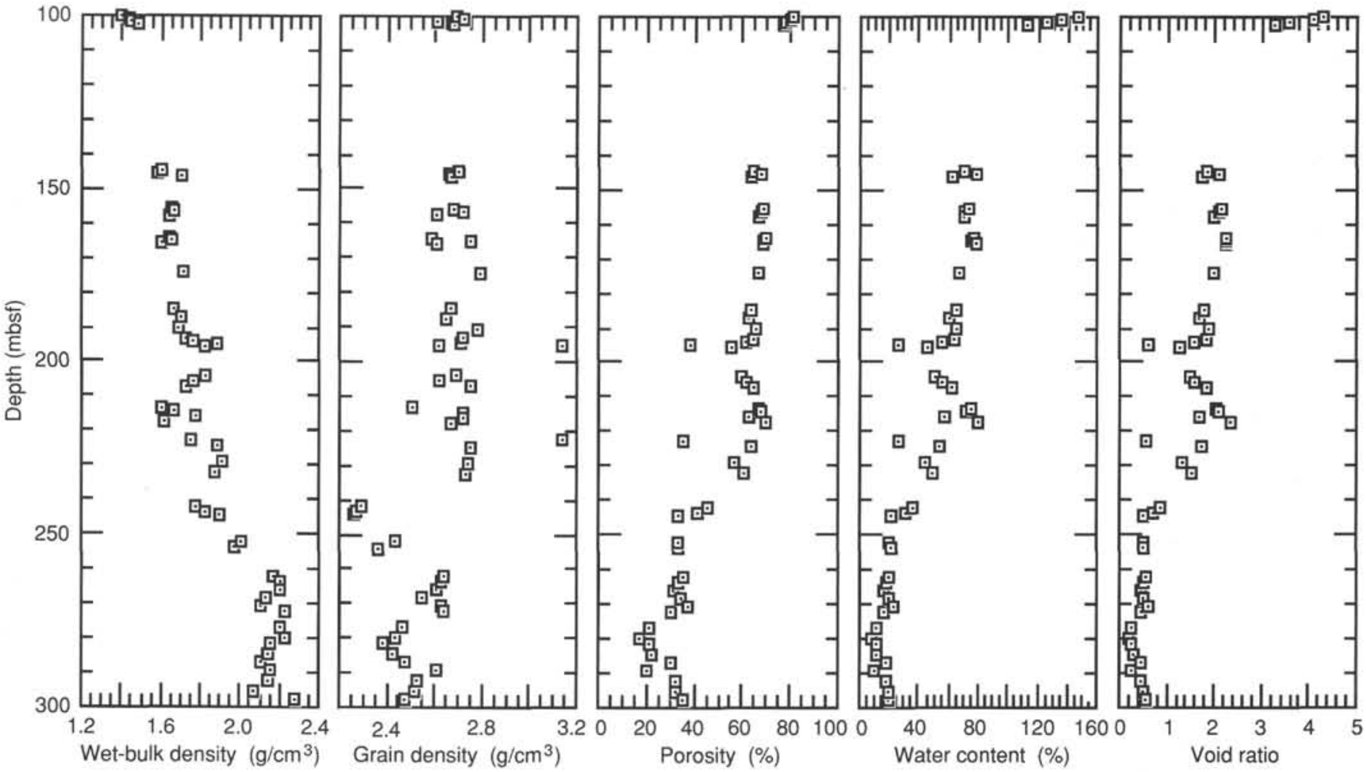

Figure 11. Downhole changes in index properties (wet-bulk density, grain density, porosity, water content, and void ratio), Hole 771A.

SEISMIC STRATIGRAPHY

Site 771 is located on multichannel seismic Line S049-05 (Fig. 13) acquired on board the *Sonne* in April 1987 and processed by the Bundesanstalt für Geowissenschaften und Rohstoffe (BGR) in February 1988 (see Hinz and Block, this volume). In addition, a pre-site, single-channel seismic reflection line was shot along the BGR line prior to drilling on 1 January 1989 aboard the *JOIDES Resolution* (Fig. 14; see also "Underway Geophysics" chapter, this volume). *Sonne* navigation was obtained with transit satellites, Loran C, and doppler sonar. The *JOIDES Resolution* used TRANSIT satellite fixes for positioning.

The site is located at 2859 m water depth on a flat plateau 1500 m above Site 768 in the Sulu Basin. The site is located on a slightly dipping terrace on the southeast side of the Cagayan Ridge. Northwest of the site, the slope is bounded by a valley and related terraces, which are interpreted as the trace of an active submarine channel (Fig. 15).

At Site 771, the acoustic basement is covered by 235 m of marl that could represent the uppermost seismic sequence (Unit 1 on Fig. 16). It is characterized on Line SO49-05 by moderately coherent seismic reflectors, parallel to the acoustic basement, whereas the seismic sequence on the *JOIDES Resolution* line is transparent and homogeneous. Northwest of the site on Line SO49-05, two distinct seismic subunits are differentiated in Unit 1. Seismic Subunit 1A is 0.2 ms thick and is much more reflective than lower Subunit 1B. Subunit 1A was interpreted to correspond to Cores 124-771A-1R and -2R.

The acoustic basement at Site 771 is marked by strong reflectors of moderate amplitude but with no clear internal structure. Immediately northwest of the site along Line S049-05 (Fig. 15), reflectors are nearly horizontal and subparallel. A preliminary interpretation made by Hinz et al. (BGR unpubl. rept. 103.463, 1988) shows this unit (Unit 2 on Fig. 16) to be deposited over large tilted blocks that face south or southeastward. If this interpretation is correct, it could indicate that Unit 2, which was identified as dominantly volcaniclastic at Site 771 (see "Lithostratigraphy" section, this chapter), postdates the extensional event affecting Unit 3. The nature of these tilted blocks remains unknown, but the blocks could correspond to a volcanic arc that rifted during the opening of the Sulu Basin or to stretched continental crust similar to that observed along the drifted margin of the South China Sea in Reed Bank and Dangerous Grounds.

SUMMARY AND CONCLUSIONS

Site 771 on the Cagayan Ridge was drilled 2859 mbsl to a depth of 304.1 mbsf. The objectives at this site were to test the age of cessation of volcanism found at Site 769, to determine whether the coarse tuffs and lapillistones at Site 769 were a widespread or a local phenomenon, and to obtain better biostratigraphic correlation between different siliceous and calcareous microfaunas and floras at a site above the CCD. Two lithologic units were distinguished at Site 771: a nannofossil marl and clay, overlying massive lapillistone, tuff, and basalt flows.

Unit I (100–233.9 mbsf) is middle Miocene to late Pliocene in age and consists of nannofossil clay and marl with rare, thin carbonate turbidites. The material also contains minor silt-size volcanic detritus. Dispersed volcanic ash is found in the lower 30 m of Unit I, and its concentration increases in the lower 2 m.

Unit II (233.9–303.0 mbsf) is late early to early middle Miocene in age. It consists of volcaniclastic strata underlain and capped by basaltic lava flows. Thin-bedded coarse to fine tuffs occur below the upper basalt, but the dominant volcaniclastic rock is massive and structureless lapillistone.

The intercalation of flows and pyroclastic deposits suggests proximity to a volcanic vent or set of vents. The hemipelagic marlstone just above the upper basalt is evidence for the submarine eruption of the lavas. The boundary between Units I and II

Table 6. Index property data, Site 771.

Core, section, interval (cm)	Depth (mbsf)	Wet-bulk density (%)	Grain density (%)	Porosity (%)	Water content (%)	Void ratio
124-771A-						
1R-1, 24–26	100.24	1.39	2.69	81.1	147.6	4.29
1R-1, 99–101	100.99	1.43	2.72	80.2	135.8	4.06
1R-2, 24–26	101.74	1.44	2.61	78.2	125.6	3.59
1R-2, 99–101	102.49	1.48	2.68	76.5	112.4	3.26
2R-1, 24–26	144.94	1.61	2.70	64.7	69.9	1.83
2R-1, 99–101	145.69	1.58	2.66	67.8	78.8	2.10
2R-2, 24–26	146.44	1.70	2.67	63.8	62.4	1.76
3R-1, 135–137	155.95	1.65	2.68	68.4	73.6	2.16
3R-2, 48–50	156.58	1.67	2.72	67.5	70.5	2.08
3R-3, 12–14	157.72	1.64	2.61	66.6	70.9	1.99
4R-1, 10–12	164.30	1.64	2.59	69.2	76.5	2.25
4R-1, 82–84	165.02	1.65	2.75	69.1	75.2	2.24
4R-1, 133–135	165.53	1.61	2.61	69.1	78.2	2.23
5R-1, 18–20	174.08	1.71	2.79	66.8	66.7	2.01
6R-1, 102–104	184.62	1.67	2.67	64.1	64.5	1.78
6R-3, 102–104	187.62	1.70	2.65	62.8	61.1	1.69
6R-5, 102–104	190.62	1.69	2.78	65.4	66.0	1.89
6R-7, 61–63	193.21	1.73	2.72	65.1	63.0	1.86
7R-1, 100–102	194.20	1.76	2.71	61.5	55.9	1.60
7R-2, 40–42	195.10	1.88	3.14	38.8	26.9	0.63
7R-2, 100–102	195.70	1.82	2.62	55.9	45.8	1.27
8R-1, 110–112	204.00	1.82	2.69	59.3	50.2	1.46
8R-2, 110–112	205.50	1.76	2.62	61.4	55.5	1.59
8R-3, 110–112	207.00	1.73	2.75	65.1	62.6	1.86
9R-1, 56–58	213.16	1.60	2.51	67.0	75.0	2.03
9R-2, 56–58	214.66	1.66	2.72	67.4	71.2	2.07
9R-3, 56–58	216.16	1.78	2.72	62.6	56.4	1.67
9R-4, 56–58	217.66	1.62	2.67	70.2	79.6	2.35
10R-1, 50–52	222.80	1.75	3.14	35.4	26.1	0.55
10R-2, 69–71	224.49	1.88	2.75	63.8	53.4	1.76
10R-5, 94–96	229.24	1.91	2.74	56.9	44.0	1.32
11R-1, 26–28	232.26	1.87	2.73	60.3	49.4	1.52
12R-1, 54–56	242.24	1.77	2.29	45.8	36.0	0.85
12R-2, 31–33	243.40	1.82	2.27	41.9	30.9	0.72
12R-2, 134–136	244.43	1.90	2.26	33.1	21.7	0.50
13R-1, 62–64	251.92	2.01	2.43	33.3	20.4	0.50
13R-2, 115–117	253.95	1.97	2.36	33.2	20.9	0.50
14R-2, 28–30	262.18	2.17	2.64	34.9	19.7	0.54
14R-3, 86–88	263.88	2.21	2.63	33.0	18.1	0.49
15R-1, 28–30	265.78	2.21	2.61	31.2	16.9	0.45
15R-3, 26–28	268.23	2.13	2.55	34.5	19.8	0.53
15R-4, 97–99	270.44	2.11	2.63	37.6	22.3	0.60
15R-5, 124–126	272.21	2.23	2.64	30.7	16.4	0.44
16R-2, 74–76	277.00	2.21	2.47	21.4	11.0	0.27
16R-4, 82–84	279.83	2.23	2.43	16.9	8.4	0.20
16R-6, 48–50	281.62	2.15	2.38	20.8	11.0	0.26
16R-8, 64–66	284.42	2.14	2.42	22.4	12.0	0.29
17R-2, 67–69	286.97	2.11	2.48	30.7	17.5	0.44
17R-4, 27–29	288.87	2.15	2.61	19.9	10.4	0.25
17R-6, 99–101	292.01	2.14	2.53	32.1	18.2	0.47
18R-1, 85–87	295.25	2.07	2.52	32.8	19.3	0.49
18R-3, 98–100	297.36	2.28	2.48	35.8	19.2	0.56

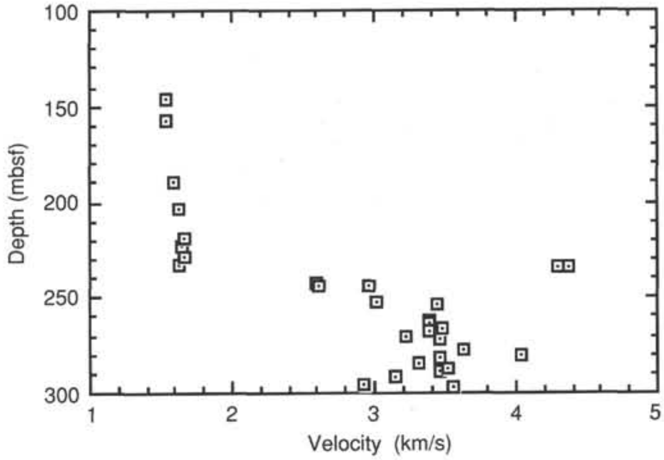

Figure 12. Hamilton Frame compressional velocity vs. depth, Hole 771A.

Table 7. Compressional wave velocity data, Site 771.

Core, section, interval (cm)	Depth (mbsf)	Velocity (km/s)
124-771A-		
2R-2, 20–22	146.40	1.53
3R-2, 137–139	157.47	1.54
6R-5, 44–46	190.04	1.60
8R-1, 88–90	203.78	1.64
9R-5, 10–12	218.70	1.66
10R-1, 50–52	222.80	1.65
10R-5, 94–96	229.24	1.68
11R-1, 26–28	232.26	1.62
11R-2, 74–76	234.24	4.29
11R-3, 6–8	234.52	4.37
12R-1, 54–56	242.24	2.60
12R-2, 31–33	243.40	2.61
12R-2, 134–136	244.43	2.96
13R-1, 62–64	251.92	3.01
13R-2, 115–117	253.95	3.45
14R-2, 28–30	262.18	3.38
14R-3, 86–88	263.88	3.39
15R-1, 28–30	265.78	3.49
15R-3, 26–28	268.23	3.39
15R-4, 97–99	270.44	3.23
15R-5, 124–126	272.21	3.47
16R-2, 74–76	277.00	3.64
16R-4, 82–84	279.83	4.03
16R-6, 48–50	281.62	3.46
16R-8, 64–66	284.42	3.31
17R-2, 67–69	286.97	3.52
17R-4, 27–29	288.87	3.47
17R-6, 99–101	292.01	3.16
18R-1, 85–87	295.25	2.92
18R-3, 98–100	297.36	3.55

represents a rapid transition from volcaniclastic to hemipelagic sedimentation in early middle Miocene time.

The major increase in the carbonate content of the cores at Sites 768, 769, and 771 near the end of the Pliocene indicates a rapid drop in the CCD. The low carbonate and high CCD in the late Miocene and early Pliocene may be the result of the closing off of the Sulu Basin because of collisions. The drop of the CCD in the Pliocene-Pleistocene may indicate variations in depth of the sills present between Mindoro and North Palawan or along the Sulu archipelago where a recent volcanic arc was built. In addition, this corresponds to a global deepening of the CCD recognized in all the major oceans at that time.

The eruption of the tuffs and lapillistones corresponds closely in time with the opening of the Sulu Sea, as shown by formation of the crust at Site 768 in the early middle Miocene. The radiolarian assemblage overlying the pyroclastic rocks at Site 768 is about the same age as that found overlying the tuffs at Sites 769 and 771; but the gross composition of the volcanic materials are different (rhyolitic vs. andesitic), so we are not sure of the parentage of the Site 768 pyroclastics.

The tuffs on the Cagayan Ridge may represent the last stage of arc volcanism for this ridge, or they may correspond to a short volcanic event that resulted from passive margin rifting (analogous to that observed on the Voring Plateau). On the basis of a roughly similar seismic reflection signature and visual descriptions of the drilled material, neither hypothesis can yet be disregarded. Compared with Site 768, the sediments overlying the brown clay are characterized by a lack of turbidites, illustrating that the present elevated position of the Cagayan Ridge was similarly elevated during all of the Neogene.

REFERENCES

Berggren, W. A., Kent, D. V., and Van Couvering, J. A., 1985. The Neogene: Part 2, Neogene geochronology and chronostratigraphy. *In* Snelling, N. J. (Ed.), *The Chronology of the Geological Record.* Geol. Soc. Mem. (London), 10:211-260.

Pearce, J. A., 1982. Trace element characteristics of lavas from destructive plate boundaries. *In* Thorpe, R. S. (Ed.), *Andesites: Orogenic Andesites and Related Rocks*: New York (Wiley-Interscience), 525-548.

Martini, E., 1971. Standard Tertiary and Quaternary calcareous nannoplankton zonation. *In* Farinacci, A. (Ed.), *Proceedings of the Second International Conference on Planktonic Microfossils, Roma, 1970*: Rome (Tecnoscienza), 2:739-785.

Riedel, W. R., and Sanfilippo, A., 1978. Stratigraphy and evolution of tropical Cenozoic radiolarians. *Micropaleontology*, 23:81-96.

Ms 124A-114

NOTE: All core description forms ("barrel sheets") and core photographs have been printed on coated paper and bound as Section 3, near the back of the book, beginning on page 423.

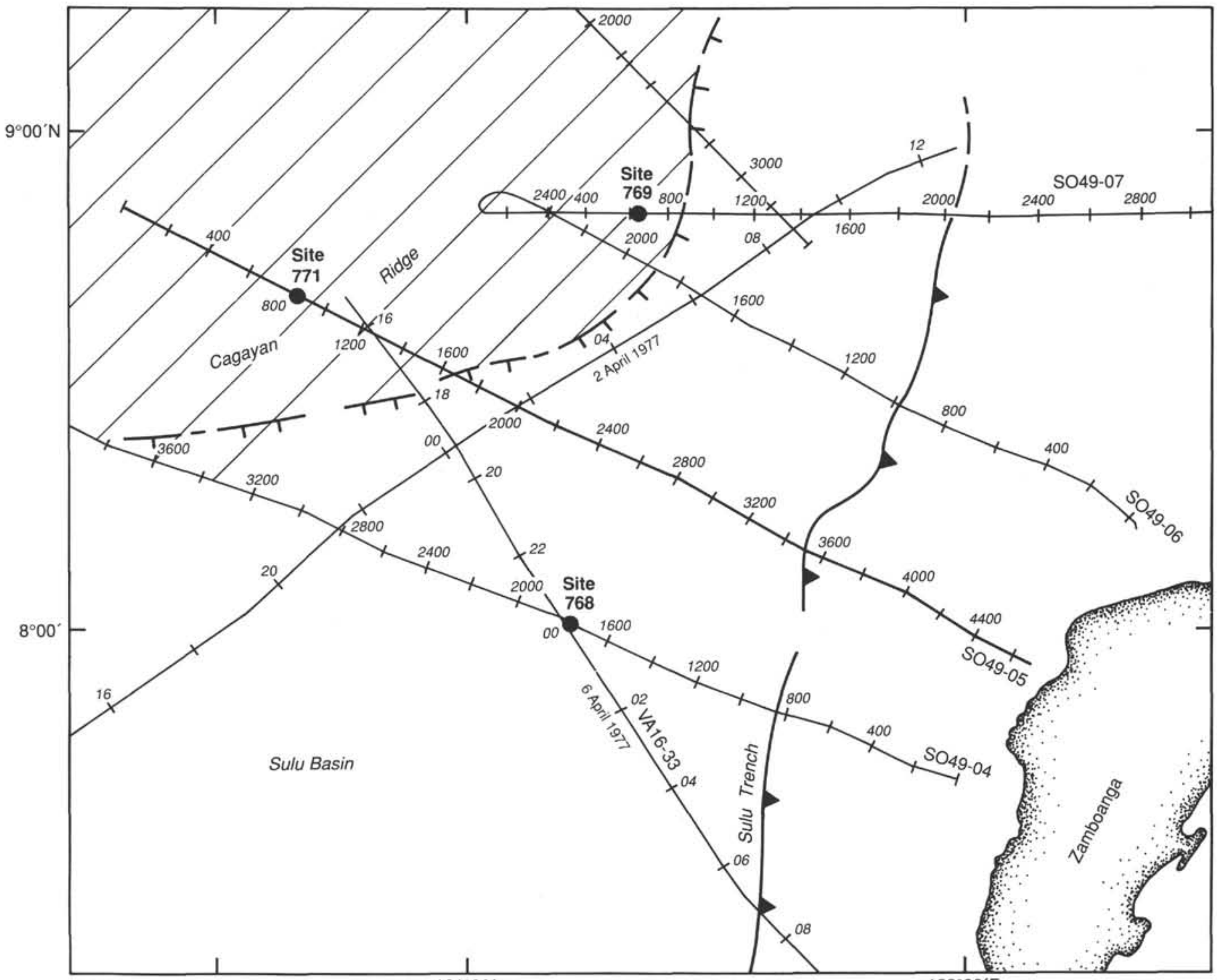

Figure 13. Location of Bundesanstalt für Geowissenschaften und Rohstoffe (BGR) seismic lines in the drilling area of Site 771. Diagonal lines indicate Cagayan Ridge.

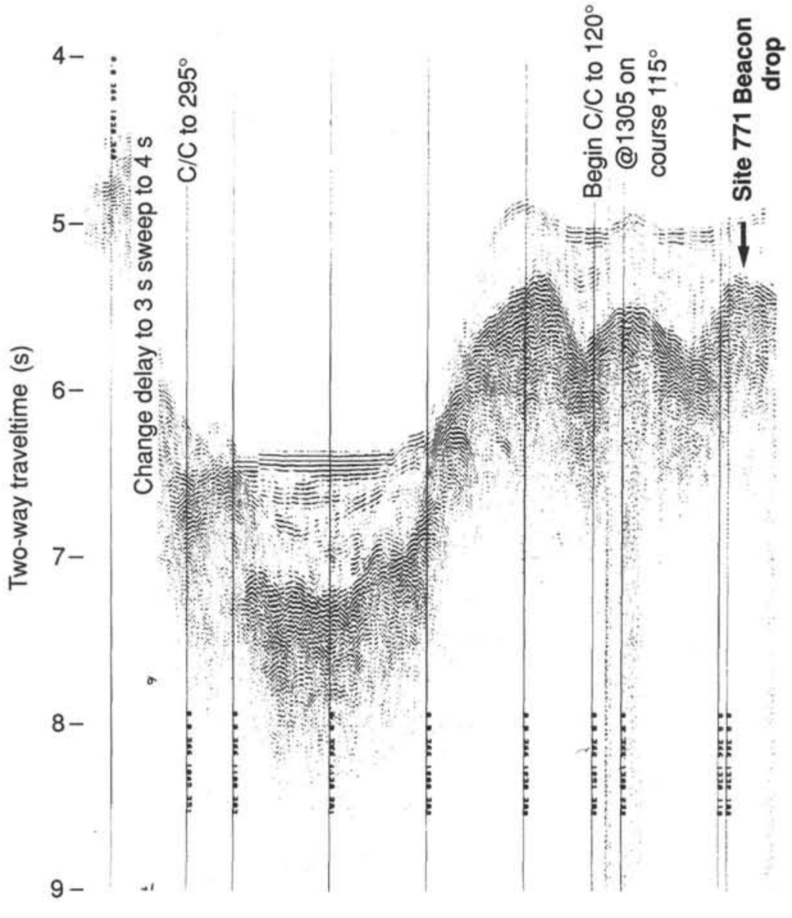

Figure 14. Single-channel seismic profile acquired during the survey of Site 771 on board *JOIDES Resolution*.

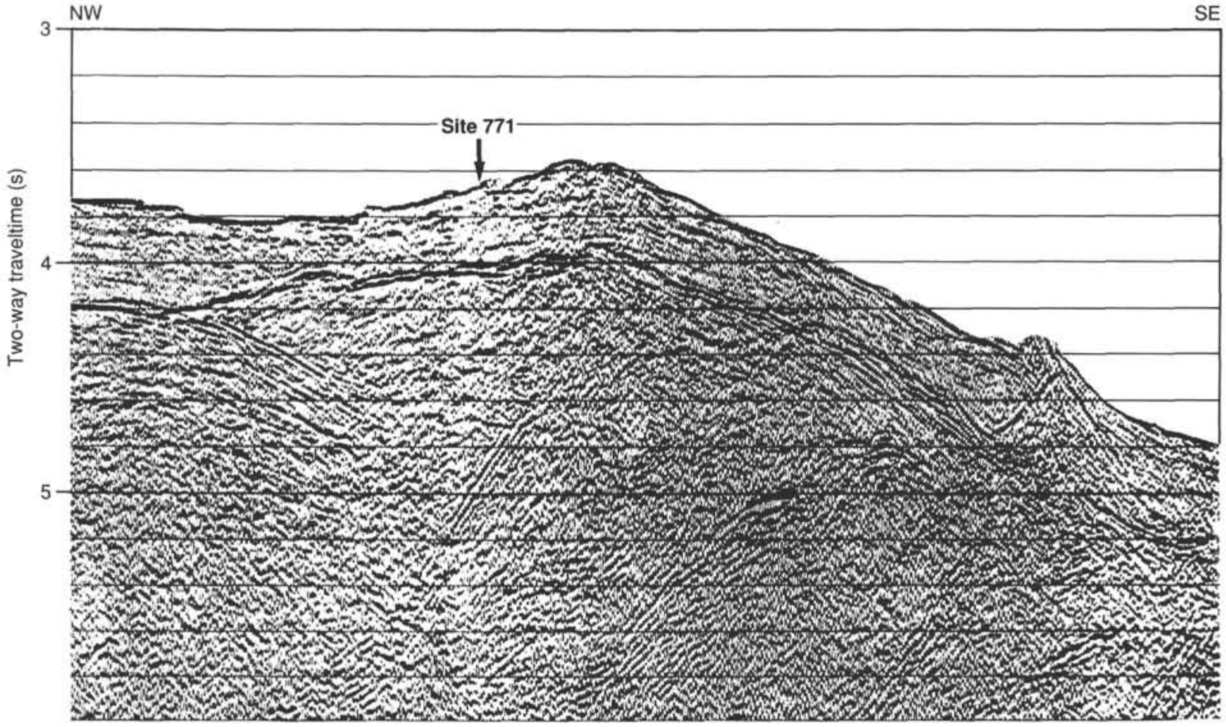

Figure 15. Migrated multichannel seismic profile of Line SO49-05 with the location of Site 771.

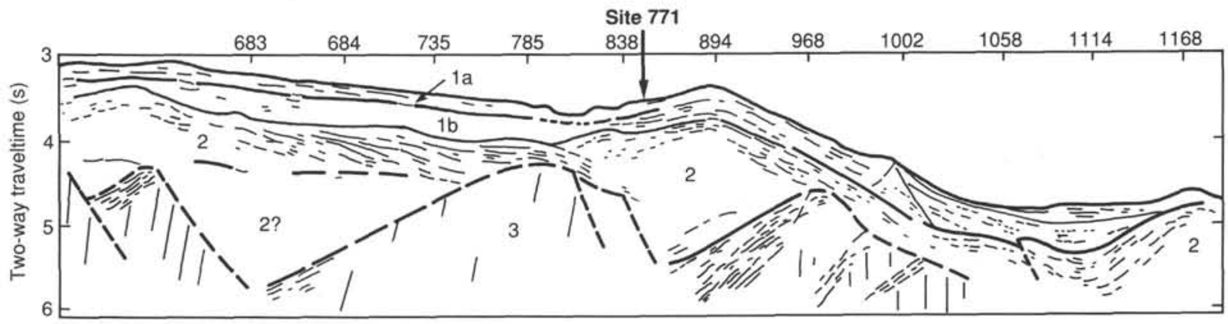

Figure 16. Part of Line SO49-05 interpreted from Hinz et al. (BGR unpubl. rept. 103.463, 1988). See text for discussion.